Enhancement of microwave emission in magnetic tunnel junction oscillators through in-plane field orientation

Z. M. Zeng,[1,a)] P. Upadhyaya,[2] P. Khalili Amiri,[2] K. H. Cheung,[1] J. A. Katine,[3] J. Langer,[4] K. L. Wang,[2] and H. W. Jiang[1]
[1]*Department of Physics and Astronomy, University of California, Los Angeles, California 90095, USA*
[2]*Department of Electrical Engineering, University of California, Los Angeles, California 90095, USA*
[3]*Hitachi Global Storage Technologies, San Jose, California 95135, USA*
[4]*Singulus Technologies, Kahl am Main, Germany*

(Received 4 April 2011; accepted 26 June 2011; published online 19 July 2011)

We observe giant enhancement of microwave emission in MgO-based magnetic tunnel junction nano-oscillators through in-plane magnetic field orientation. At an optimal in-plane field angle, the output power reaches up to 240 nW, two orders of magnitude higher compared to the vicinity of the easy axis (~1 nW). Moreover, in this condition, the linewidth is significantly narrowed (<100 MHz) and the additional precession modes are suppressed. Analysis of the data indicates that the optimal field angle is influenced by the field-like torque. The results demonstrate that controlling the in-plane magnetic field orientation can be an important strategy for developing high-power spin-torque oscillators. © *2011 American Institute of Physics*. [doi:10.1063/1.3613965]

Spin-transfer torque (STT) induced by spin-polarized current[1,2] can lead to a direct coupling between transport and local magnetization in a nanomagnet, exciting a steady precession of the magnetization.[3,4] This phenomenon enables a nanosized oscillator, i.e., spin-torque nano-oscillator (STNO), which is tunable over a wide frequency range by varying the applied dc current or magnetic field. A substantial amount of experimental research[5–11] has been carried out on different types of STNOs, but the relatively low output power is still a main challenge for a majority of practical applications. Recently, MgO-based magnetic tunnel junction (MTJ) STNOs with large tunnel magnetoresistance (MR) were shown to deliver large output power, e.g., 140 nW in Ref. 12 and 175 nW in Ref. 13. However, the STNOs described in these reports also exhibited multiple emission peaks[12] and large linewidths.[12,13] Thadani *et al.*[7] and Mizushima *et al.*[10] reported that the application of the magnetic field near/along the magnetic hard axis of the nanopillars can narrow the linewidth. However, the output power in their STNOs was quite low (< 1 nW). In this letter, we report that both large output power and narrow linewidth, along with the suppression of additional precession modes, can be simultaneously achieved in MgO-based STNOs by optimizing the in-plane field orientation.

MTJs with stacks of composition PtMn (15)/$Co_{70}Fe_{30}$ (2.5)/Ru (0.85)/$Co_{40}Fe_{40}B_{20}$ (2.4)/MgO (0.8)/$Co_{60}Fe_{20}B_{20}$ (1.8) (thickness in nm) were deposited using a Singulus TIMARIS PVD system and annealed at 300 °C for 2.0 h in a magnetic field of 1 T. The films were subsequently patterned into ellipse-shaped pillars. While similar results have been obtained on a variety of samples, measurements will be presented here only for devices with nominal dimensions of 140 nm × 85 nm. We performed all measurements at room temperature, with an in-plane magnetic field applied using a projected field electromagnet that allows us to control the field angle continuously.[14] The MR ratio and the resistance-area product in the parallel (P) state were ~120% and 2.8 Ω μm^2, respectively. The coupling or interaction field (H_{int}, favoring the *P* state) between the free layer and pinned layer was found to be ~100 Oe as shown in Fig. 1(a). The in-plane field angle (θ_H) was calibrated by considering the combination of external field (H_{ext}) and H_{int} [see inset in Fig. 2(b)]. The microwave emissions were studied by applying H_{ext} and sweeping the dc current (I_{dc}) from 0 to 1.5 mA (corresponding current density $J = 1.6 \times 10^7$ A/cm^2, where a positive current is defined as electrons flowing from the pinned layer to the free layer). At each current value, microwave measurements up to 8.0 GHz were recorded on a spectrum analyzer after 26 dB amplification. The background noise, measured at zero dc current, was subtracted from the power spectra.

In Figures 2(a) and 2(b), we display microwave emission contours as a function of in-plane field angle θ_H on a logarithmic scale, as well as microwave emission spectra at $\theta_H = 22°$, 62°, and 90°. It can be seen that the microwave signals vary strongly as a function of θ_H and that three distinct regions are present.

1. $0° \le \theta_H < 50°$, microwave signals display an increasing fundamental (first) peak power, a decreasing second harmonic peak power, and an obvious low-frequency noise.

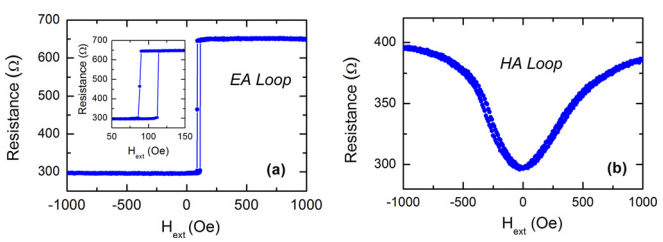

FIG. 1. (Color online) Resistance as a function of in-plane field H_{ext} for the same device for fields (a) along the easy-axis direction and (b) along the hard-axis direction. Inset in (a) is the magnified view in the low-field range.

a)Author to whom correspondence should be addressed. Electronic mail: zhongming.zeng@gmail.com.

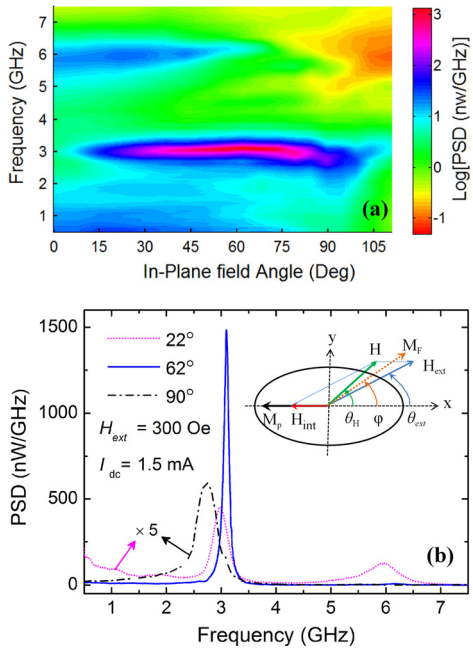

FIG. 2. (Color online) (a) Power spectral density (PSD) plotted on a logarithmic scale as a function of in-plane field angle θ_H. (b) PSD for field angles $\theta_H = 22°$, 62°, and 90°. All spectra were recorded with $H_{ext} = 300$ Oe and $I_{dc} = 1.5$ mA. Inset in (b): directions of the external field (H_{ext}) and the free-layer magnetization (M_f). The in-plane field angle θ_H is calibrated by considering the coupling field (H_{int}), thus $\theta_H > \theta_{ext}$. Here H is the vector sum of H_{ext} and H_{int}.

The increasing power suggests that the precession amplitude grows as a function of θ_H at fixed current, and the reduction of low-frequency noise indicates that the dynamics become more coherent as θ_H increases. This is consistent with the observation of multiple peaks and a large low-frequency noise in Ref. 12, where the field orientation is near the easy axis.

2. $50° \leq \theta_H < 80°$, in this region, the power of the first peak reaches a maximum while the second peak almost disappears. In particular, when θ_H is ~62°, the microwave signal has the narrowest spectral line, a drastic increase in the power, and a single-mode spectrum with a disappearance of low-frequency noise, suggesting coherent oscillations.[15,16] At $I_{dc} = 1.5$ mA, the peak linewidth is 98 MHz and the integrated power reaches up to 240 nW, two orders of magnitude higher than that near the easy-axis direction (≈1 nW). This value is larger than the highest values reported so far (175 nW in Ref. 13). More importantly, the STNOs in this work show narrower linewidth and suppression of the additional precession modes, which are critical for practical applications. The linewidth is found to further decrease with increase of the bias current, e.g., at $I_{dc} = 1.8$ mA, the linewidth was narrowed to ~60 MHz. To avoid damaging the devices, all data presented here were collected at $I_{dc} = 1.5$ mA or below.
3. $\theta_H \geq 80°$, where the power drops abruptly and the linewidth increases dramatically.

Our results show qualitatively different behavior from the previously reported works,[7,10] where the peak frequency and linewidth of the microwave signals decrease monotonously as the in-plane field orientation moves towards hard-axis direction. In our case, the peak frequency decreases gradually as θ_H increases and reaches a minimum at $\theta_H = 90°$ [see Fig. 3(a)] due to the effect of the in-plane shape anisotropy[17,18] only at low currents (e.g., $I_{dc} = 0.5$ and 0.75 mA). However, the frequency variations with θ_H become small at high currents, e.g., the frequency exhibits almost no change from $\theta_H = 0°$ to $\theta_H = 80°$ at $I_{dc} = 1.5$ mA. The linewidth variation with θ_H is also strongly dependent on the dc current as shown in Fig. 3(c), i.e., the variations are irregular for small currents ($I_{dc} < 1.0$ mA), while there is a minimum at $\theta_H \approx 60°$ for larger currents ($I_{dc} > 1.0$ mA). Furthermore, the output power of up to 240 nW shows significant enhancement compared to the previously reported results (less than 1 nW in Refs. 7 and 10). The large power is ascribed to the high MR ratio (~120%) and the large oscillation amplitude, which is verified by time-domain measurements, reaching up to 9.0 mV (peak-to-peak, not shown here). Second, a qualitative difference can also be seen in the power variations with θ_H in our case. In metallic STNOs, the maximum power was found near the hard-axis direction, while the power variation with θ_H is irregular for various dc currents.[7] In MgO MTJ based STNOs reported by Mizushima *et al.*, the power only showed a change by a factor of ~2 with θ_H.[10] In their further study,[11] the distinct microwave peaks were only present at $\theta_H \approx 40°$ and the authors attributed them to nonuniform oscillation modes, while uniform modes are observed in our STNOs. Moreover, the output power in our STNOs shows clear angular dependence for each dc current and the θ_H value corresponding to the maximum power is related to the current values, rather than occurring at the hard-axis direction.

We propose here two factors that are believed to contribute to the observed variations with in-plane filed angle. First, it has been shown that the spin torque L depends on the angle φ between the magnetizations of the free and pinned layers and the asymmetry parameter Λ.[19] The spin torque magnitude is the largest at $\varphi = 90°$ for the symmetric case ($\Lambda = 1$). However, our structure is not symmetric since the pinned layer is $Co_{40}Fe_{40}B_{20}$ while the free layer is Co-rich $Co_{60}Fe_{20}B_{20}$, resulting in the maximum spin torque L occurring away from the angle $\varphi = 90°$. The large spin torque can result in large-amplitude oscillations, further producing high output power.[20] Therefore, the maximum power positions are at a certain angle θ_H rather than at the hard-axis direction. Second, the dynamics may be affected by perpendicular spin torque ($\tau_\perp$, i.e., field-like torque),[21] since in MTJs, the $\tau_\perp$ is strong (up to 30% of the in-plane torque[12]) while negligible in the metallic devices.[22] The field-like torque acts as an additional field, whose contribution may push the free layer magnetization toward the hard-axis direction, i.e., increasing the actual magnetization angle φ [$(H_{eff} - H_k)\cos\varphi = H\cos\theta_H - b_j$,[23,24] where H_{eff} is the effective field acting on the free-layer magnetization, H_k is the in-plane anisotropy, and b_j is the effective field due to the perpendicular spin torque]. As mentioned above, the maximum power occurs at a certain angle φ, thus at a given φ, the in-plane field angle θ_H for achieving the maximum power decreases with increasing the dc current (assuming that b_j increases with dc current). In other words, the maximum power position shifts to lower in-plane field angles as shown in Fig. 3(d). For example, the maximum power is observed

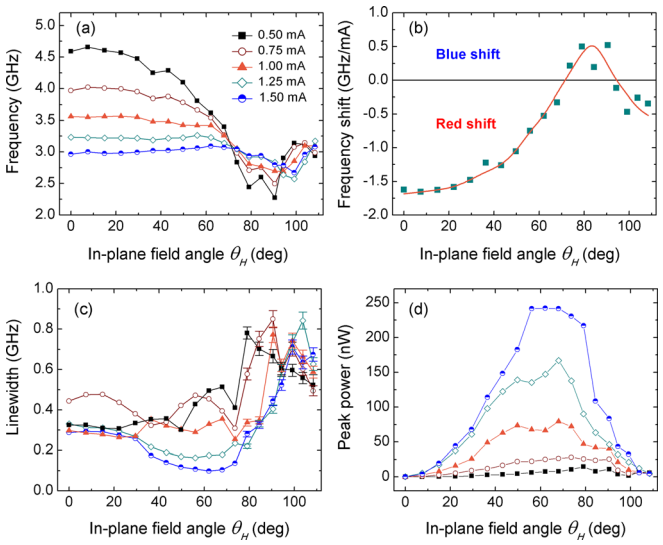

FIG. 3. (Color online) (a) Frequency, (b) frequency shift, (c) linewidth, and (d) integrated power of the first peak as a function of in-plane field angle θ_H. The solid curve in (c) is added as a guide for the viewer.

at $\theta_H \approx 62°$ for $I_{dc} = 1.5$ mA while at $\theta_H \approx 80°$ for $I_{dc} = 0.5$ mA. However, for the quantitative analysis of the $\tau_\perp$ effect on STNOs, more theoretical work is still required. Nevertheless, our data suggest that the field-like torque in MTJ STNOs plays a significant role in STT-driven magnetization dynamics.

Finally, we turn to the angular dependence of the linewidth. According to nonlinear auto-oscillator theory, the linewidth (Δf) in the above threshold regime can be written as[16]

$$\Delta f = \Gamma_0 (k_B T / E_0)[1 + (N/\Gamma_{eff})^2], \quad (1)$$

where Γ_0 is the linear relaxation rate, k_B is the Boltzmann constant, T is the absolute temperature, E_0 is the oscillator energy that increases with the output power P, N is the nonlinearity coefficient, and Γ_{eff} is the effective nonlinear damping. It can be seen from Eq. (1) that, for a given dc current, the linewidth depends on the output power P and the nonlinearity related to the nonlinear frequency shift coefficient N. The angular dependence of the frequency shift is shown in Fig. 3(b). At $\theta_H = 70°$ or 95°, the frequency shift is zero, which indicates the nonlinear effect is negligible ($N = 0$) in these conditions. However, these two conditions do not yield the narrowest linewith. Especially at $\theta_H = 95°$, although the nonlinearity is close to zero, the linewidth is relatively large due to low power corresponding to small-amplitude oscillation. This is reasonable since the small-amplitude dynamics are strongly influenced by thermal fluctuations.[25,26] The narrowest linewidth is observed at $\theta_H \approx 60°$ for $I_{dc} = 1.5$ mA [see Fig. 3(c)] where the power is the highest while N is nonzero. This suggests that the output power is dominant in determining the linewidth in our STNOs.

In summary, we have shown microwave emissions with large power, narrow linewidth, and the suppression of the additional precession modes in MgO-based STNOs. The maximum power reaches up to 240 nW together with a linewidth of 98 MHz at $\theta_H = 62°$ and $I_{dc} = 1.5$ mA. We attribute this dramatic enhancement to the suppression of the nonuniform precession modes of the free layer. In addition, our results suggest that the optimal θ_H corresponding to the maximum power is affected by the field-like torque. Our data demonstrate that controlling the in-plane magnetic field orientation is important for the development of high-power STNOs for microwave applications.

We would like to acknowledge our fruitful conversations with Professor A. Slavin, Professor I. N. Krivorotov, Dr. Y. Huai, and J. G. Alzate. This work was supported by the DARPA STT-RAM program and the Nanoelectronics Research Initiative (NRI) through the Western Institute of Nanoelectronics (WIN).

[1] L. Berger, Phys. Rev. B **54**, 9353 (1996).
[2] J. C. Slonczewski, J. Magn. Magn. Mater. **159**, L1 (1996).
[3] S. I. Kiselev, J. C. Sankey, I. N. Krivorotov, N. C. Emley, R. J. Schoelkopf, R. A. Buhrman, and D. C. Ralph, Nature **425**, 380 (2003).
[4] W. H. Rippard, M. R. Pufall, S. Kaka, S. E. Russek, and T. J. Silva, Phys. Rev. Lett. **92**, 027201 (2004).
[5] S. Kaka, W. H. Rippard, M. R. Pufall, S. E. Russek, T. J. Silva, and J. A. Katine, Nature **437**, 389 (2005).
[6] F. B. Mancoff, N. D. Rizzo, B. N. Engel, and S. Tehrani, Nature **437**, 393 (2005).
[7] K. V. Thadani, G. Finocchio, Z.-P. Li, O. Ozatay, J. C. Sankey, I. N. Krivorotov, Y.-T. Cui, R. A. Buhrman, and D. C. Ralph, Phys. Rev. B **78**, 024409 (2008).
[8] A. V. Nazarov, H. M. Olson, H. Cho, K. Nikolaev, Z. Gao, S. Stokes, and B. B. Pant, Appl. Phys. Lett. **88**, 162504 (2006).
[9] D. Houssameddine, S. H. Florez, J. A. Katine, J.-P. Michel, U. Ebels, D. Mauri, O. Ozatay, B. Delaet, B. Viala, L. Folks, B. D. Terris, and M.-C. Cyrille, Appl. Phys. Lett. **93**, 022505 (2008).
[10] K. Mizushima, T. Nagasawa, K. Kudo, Y. Saito, and R. Sato, Appl. Phys. Lett. **94**, 152501 (2009).
[11] K. Kudo, T. Nagasawa, R. Sato, and K. Mizushima, Appl. Phys. Lett. **95**, 022507 (2009).
[12] A. M. Deac, A. Fukushima, H. Kubota, H. Maehara, Y. Suzuki, S. Yuasa, Y. Nagamine, K. Tsunekawa, D. D. Djayaprawira, and N. Watanabe, Nat. Phys. **4**, 803 (2008).
[13] Y. Masugata, S. Ishibashi, H. Tomita, T. Seki, T. Nozaki, Y. Suzuki, H. Kubota, A. Fukushima, and S. Yuasa, J. Phys.: Conf. Ser. **266**, 012098 (2011).
[14] See http://www.gmw.com/electromagnets/Miniature/5201/5201.html for GMW Projected Field Electromagnet.
[15] J.-V. Kim, Phys. Rev. B **73**, 174412 (2006).
[16] J.-V. Kim, Q. Mistral, C. Chappert, V. S. Tiberkevich, and A. N. Slavin, Phys. Rev. Lett. **100**, 167201 (2008).
[17] V. Tiberkevich, I. N. Krivorotov, G. Gerhart, and A. Slavin, J. Magn. Magn. Mater. **321**, L53 (2009).
[18] A. N. Slavin and V. S. Tiberkevich, IEEE Trans. Magn. **45**, 1875 (2009).
[19] J. C. Slonczewski, J. Magn. Magn. Mater. **247**, 324 (2002).
[20] I. N. Krivorotov, D. V. Berkov, N. L. Gorn, N. C. Emley, J. C. Sankey, D. C. Ralph, and R. A. Buhrman, Phys. Rev. B **76**, 024418 (2006).
[21] Y. Zhou and J. Akerman, Appl. Phys. Lett. **94**, 112503 (2009).
[22] I. Theodonis, N. Kioussis, A. Kalitsov, M. Chshiev, and W. H. Butler, Phys. Rev. Lett. **97**, 237205 (2006).
[23] S. Petit, N. de Mestier, C. Baraduc, C. Thirion, Y. Liu, M. Li, P. Wang, and B. Dieny, Phys. Rev. B **78**, 184420 (2008).
[24] P. K. Muduli, O. G. Heinonen, and J. Akerman, Phys. Rev. B **83**, 184410 (2011).
[25] J. C. Sankey, I. N. Krivorotov, S. I. Kiselev, P. M. Braganca, N. C. Emley, R. A. Buhrman, and D. C. Ralph, Phys. Rev. B **72**, 224427 (2005).
[26] I. N. Krivorotov, N. C. Emley, R. A. Buhrman, and D. C. Ralph, Phys. Rev. B **77**, 054440 (2008).